Electronic Supplementary Material (ESI) for Nanoscale.

Supporting Information: Ion transport and softening in a polymerized ionic liquid

Rajeev Kumar,[*,†] Vera Bocharova,[¶] Evgheni Strelcov,[‡] Alexander Tselev,[‡] Ivan I. Kravchenko,[‡] Stefan Berdzinski,[§] Veronika Strehmel,[§] Olga S. Ovchinnikova,[¶] Joseph A. Minutolo,[‖] Joshua R. Sangoro,[‖] Alexander L. Agapov,[⊥] Alexei P. Sokolov,[¶] Sergei V. Kalinin,[‡] and Bobby G. Sumpter[‡]

Computer Science and Mathematics Division, Oak Ridge National Laboratory, Oak Ridge, TN-37831, Center for Nanophase Materials Sciences, Oak Ridge National Laboratory, Oak Ridge, TN-37831, Chemical Sciences Division, Oak Ridge National Laboratory, Oak Ridge, TN-37831, Department of Chemistry and Institute for Coatings and Surface Chemistry, Hochschule Niederrhein University of Applied Sciences, Adlerstrasse 32, D-47798 Krefeld, Germany, Department of Chemical and Biomolecular Engineering, University of Tennessee, Knoxville, TN - 37996, and Department of Chemistry, University of Tennessee, Knoxville, TN - 37996

E-mail: kumarr@ornl.gov

[*]To whom correspondence should be addressed
[†]Computer Science and Mathematics Division, Oak Ridge National Laboratory, Oak Ridge, TN-37831
[‡]Center for Nanophase Materials Sciences, Oak Ridge National Laboratory, Oak Ridge, TN-37831
[¶]Chemical Sciences Division, Oak Ridge National Laboratory, Oak Ridge, TN-37831
[§]Department of Chemistry and Institute for Coatings and Surface Chemistry, Hochschule Niederrhein University of Applied Sciences, Adlerstrasse 32, D-47798 Krefeld, Germany
[‖]Department of Chemical and Biomolecular Engineering, University of Tennessee, Knoxville, TN - 37996
[⊥]Department of Chemistry, University of Tennessee, Knoxville, TN - 37996

Modeling of the temperature distribution in an ionic polymer under an electrically biased AFM tip

The numerical modeling to estimate the temperature increase due to Joule heating of the polymer film was performed using the Joule heating module of the COMSOL finite element analysis package. Figure S1 displays a layout of the model in the vicinity of the tip apex and a map of the thermal distribution for the material parameter values are listed in Table S1. The model is two-dimensional axi-symmetric and the overall size is : radius, r, is $5\mu m$, and height is $5\mu m$. The AFM tip is modeled as a disk electrode with a radius of $100\,nm$ on top of the polymer film as shown in Figure S1. The gold layer is the bottom electrode (ground). The tip bias for the thermal distribution shown in Figure S1 was equal to 10 V. The boundary condition at all outer boundaries of the model (top of the polymer layer, bottom of the SiO_2, and all boundaries at $r = 5\mu m$) are for thermal insulation. Such boundary conditions result in overestimation of the temperature. The thermal conductivity of the polymer in Table S1 is below the lower values found in literature for similar polymers. In turn, electrical conductivity is above the upper values found in literature. This choice of parameter values results in overestimation of the polymer temperature in the model as well.

Table S1: Material parameter values used in the finite element model

	Polymer	Gold	SiO_2
Thermal conductivity, k [W/(m K)]	10^{-3}	317.6	1.4
Heat capacity, c_p, [J/(kg K)]	0.03	129	730
Electrical conductivity, σ, [S/m]	10^{-4}	4.5×10^7	0
Density, ρ, [kg/m^3]	1300	19280	2200
Relative permittivity, ε	2.5	1.0	4.2

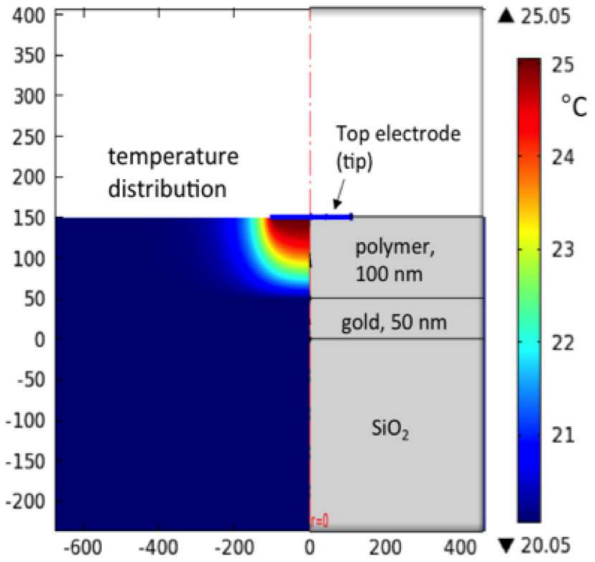

Figure S1: The right part of the figure shows a layout of the finite element model; on the left, is the temperature distribution map for the conditions as described in the text.

Estimates of ionic conductivity using scanning probe microscopy measurements

We have estimated ionic conductivity of the PolyIL films ignoring the non-linear effects resulting from the dissociation of ions. Using Ohm's law in the steady state, conductivity is given by the relation $\sigma = I(\infty)/E = I(\infty)S/SE$, where $I(\infty)$ is the steady state current *per unit area*, S is the area of the current-collecting electrode (= area of the tip in contact with the PolyIL film) and E is the applied electric field. The latter is estimated by using the relation ($E = V/L, L$ being the distance between the electrodes) and ignores non-linear effects resulting from screening. L is estimated using the Z-profiles and corrections due to plunging of the AFM tip and reduction in the distance between electrodes are included in the estimates. S is estimated to be equal to the surface area of a cylinder of the same radius as the tip ($= 25\,nm$). For the results presented in Table S2, $S = \pi r^2 + 2\pi r(300 - L)\,nm^2$ so that $r = 25\,nm$. Based on these assumptions, estimates of ionic conductivity are obtained and presented in Table S2.

Table S2: Estimates of ionic conductivity of the PolyIL using steady state parameters

Voltage V [V]	Steady state current ($I(\infty)S$) [pA]	Sample thickness L [nm]	Ionic conductivity σ, [S/m]
4	0.0679	300	2.59×10^{-6}
5	0.0658	300	2.01×10^{-6}
6	0.2477	300	6.31×10^{-6}
10	0.7029	300	1.07×10^{-5}
15	2.6144	287	1.25×10^{-5}
20	5.4201	258	8.17×10^{-6}

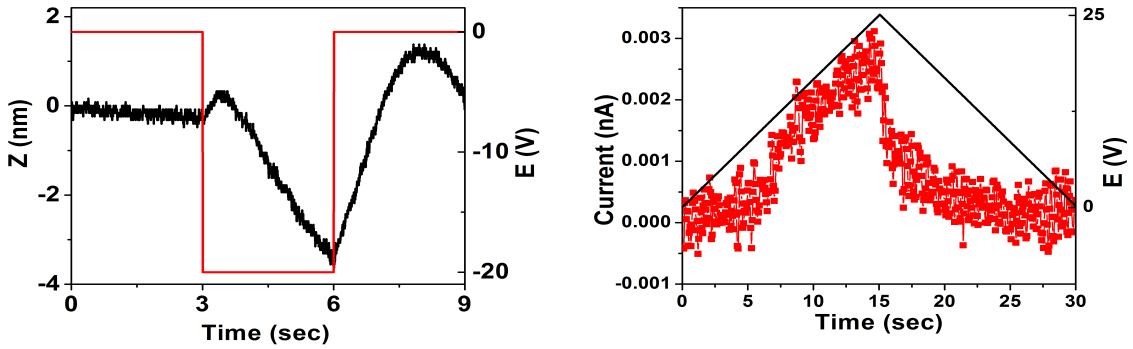

(a) (b)

Figure S2: (a) Applied voltage (red) and the Z-profile (black) for negative bias; (b) Current response (red) measured at $\sim$ 0% RH during application of the triangular bias waveform (black) with the magnitude of 25 V shows reversible nature of the current-voltage relation.

DC conductivity using broadband dielectric spectroscopy measurements

The dc conductivity (shown in Figure S3) was determined from the plateau value of the real part of the complex conductivity function as explained in Refs.[1,2] The glass transition temperature (T_g) was determined as 326 K using a Mettler-Toledo DSC 822e calorimeter with cooling and heating rates of 10 K/min.

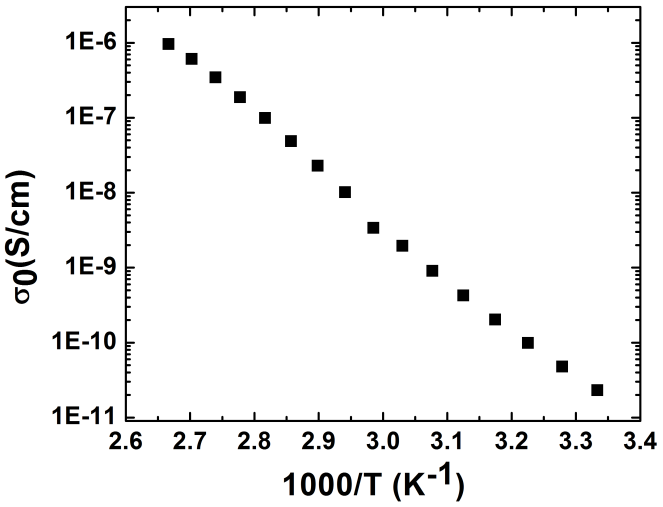

Figure S3: The dc conductivity, σ_0, of the polymerized ionic liquid measured by broadband dielectric spectroscopy as a function of the inverse temperature.

Ion transport: Poisson-Nernst-Planck (PNP) description

We have studied the kinetics of charging as well as steady state relations between ionic current and applied voltage in films of PolyILs using the Poisson-Nernst-Planck (PNP) formalism.[3] The general treatment for the ion transport in a two component system is presented below. For comparison with experiments, we have ignored the curvature of the SPM tip and calculations are done under the assumption of azimuthal symmetry. Current per unit area is computed using the PNP formalism and the area of the SPM tip is used to compute the net current.

Poisson-Nernst-Planck (PNP) formalism for a two component system

Let us consider a polymerized ionic liquid film under an applied voltage bias. Furthermore, let us assume that dominant contribution to ionic current for the film results from transport of dissociated/"free" counterions. For describing the current-voltage relation for the film, we have used the PNP formalism for a *given* counterion concentration on each side of the film. Comparison of predictions obtained from the PNP formalism with experimental current-voltage curves allows us to extract the concentration of counterions on each side of the film.

For the film under an applied voltage bias, we consider two kinds of ions, positive (cations) and negative (anions), contributing to ion transport. In the *absence of any reactions*, ion transport is governed by conservation of mass, written as continuity equation in the form

$$\frac{\partial c_i(\mathbf{r},t)}{\partial t} = -\nabla \cdot \mathbf{J}_i(\mathbf{r},t) \quad \text{for} \quad i = \pm \tag{S1}$$

where $c_i(\mathbf{r},t)$ and $J_i(\mathbf{r},t)$ are the number density (per unit volume) and flux (per unit area) of ions of type $i = \pm$ at a location described by the position vector $\mathbf{r}$ at time t, respectively. The latter is given by

$$\mathbf{J}_i(\mathbf{r},t) = -D_i \nabla c_i(\mathbf{r},t) - \xi_i c_i(\mathbf{r},t) \nabla \psi(\mathbf{r},t) \tag{S2}$$

where the first term on the right hand side quantifies contribution from diffusion and the second term is the convective part resulting from an applied electric field. D_i and ξ_i are the diffusion constant and electrophoretic mobility of ions of type i, respectively. Furthermore, $\psi(\mathbf{r},t)$ is the electrostatic potential at $\mathbf{r}$ at time t, described by the Poisson equation

$$\nabla . [\varepsilon(\mathbf{r}) \nabla \psi(\mathbf{r},t)] = -\sum_{i=\pm} z_i e c_i(\mathbf{r},t) \tag{S3}$$

where $\varepsilon(\mathbf{r})$ is the position-dependent dielectric function, z_i is the valency (with sign) of ions of type $i = \pm$ and e is the charge of an electron. Using the definition that ionic current is the flux of charges, we can write the *net local* current (per unit area) as

$$I(\mathbf{r},t) = \sum_{i=\pm} I_i(\mathbf{r},t) = \sum_{i=\pm} z_i e J_i(\mathbf{r},t) \tag{S4}$$

In principle, one should solve the Poisson equation and continuity equations with flux given by diffusion and convective terms in a self-consistent manner to describe current-voltage relations. However, in this work, we are interested in the kinetics of charge build-up due to ion transport and

extracting concentration of counterions on each side of the film by a comparison with experiments. For such purposes, we have done a linear response calculation for the kinetics of charge build-up followed by a one-dimensional steady state analysis for the current in terms of local electrostatic potential.

Kinetics of charge build up : linear response analysis

In this section, we present a linear response analysis in order to gain insight into kinetics of charge build up. The governing equations are Eqs. S1- S3, which leads to

$$\frac{\partial c_i(\mathbf{r},t)}{\partial t} = D_i\left[\nabla^2 c_i(\mathbf{r},t) + \frac{z_i e}{k_B T}\nabla.\{c_i(\mathbf{r},t)\nabla\psi(\mathbf{r},t)\}\right] \quad \text{for} \quad i=\pm \tag{S5}$$

where we have used Einstein's relation between electrophoretic mobility and diffusion constant, written as $\xi_i = z_i e D_i/k_B T$, where $k_B T$ is the Boltzmann's constant times temperature. Also, we assume that relative permittivity is independent of position (i.e., $\varepsilon(\mathbf{r}) = \varepsilon$) so that the Poisson equation becomes (cf. Eq. S3)

$$\varepsilon\nabla^2\psi(\mathbf{r},t) = -\sum_{i=\pm} z_i e c_i(\mathbf{r},t) \tag{S6}$$

Let us consider a scenario where a small voltage bias is applied, which leads to a small pertubrabtion in local concentration. For such a scenario, we can write $c_i(\mathbf{r},t) = \langle c_i\rangle + \delta c_i(\mathbf{r},t)$ so that electroneutrality is satisfied in the absence of applied bias i.e., $\sum_{i=\pm} z_i\langle c_i\rangle = 0$. Noting that $\delta c_i(\mathbf{r},t)$ and $\nabla\delta c_i(\mathbf{r},t)$ are infinitesimal in the linear response analysis, we can write (cf. Eq. S5)

$$\frac{\partial \delta c_i(\mathbf{r},t)}{\partial t} = D_i\left[\nabla^2\delta c_i(\mathbf{r},t) - \frac{z_i e}{\varepsilon_o\varepsilon k_B T}\langle c_i\rangle\left\{\sum_{i=\pm} z_i e\delta c_i(\mathbf{r},t)\right\}\right] \quad \text{for} \quad i=\pm \tag{S7}$$

where we have neglected second degree terms of the form $\delta c_i^2(\mathbf{r},t)$ and $\delta c_i(\mathbf{r}',t).\nabla\delta c_i(\mathbf{r},t)$ on the right hand side.

Let us consider two new functions constructed to decouple these two equations:

$$h(\mathbf{r},t) = \delta c_+(\mathbf{r},t) + \delta c_-(\mathbf{r},t) \tag{S8}$$

$$g(\mathbf{r},t) = \delta c_+(\mathbf{r},t) - \delta c_-(\mathbf{r},t) \tag{S9}$$

where $h(\mathbf{r},t)$ and $g(\mathbf{r},t)$ quantifies fluctuations in the total number density and charge density ($=\tilde{z}eg(\mathbf{r},t)$ so that $z_+ = -z_- = \tilde{z}$), respectively, at location $\mathbf{r}$ at time t. Eqs. S7 can be written in terms of these functions as (using $\langle c_+\rangle = \langle c_-\rangle = \langle c\rangle$)

$$\frac{\partial}{\partial t}\left[\frac{\delta c_+(\mathbf{r},t)}{D_+} + \frac{\delta c_-(\mathbf{r},t)}{D_-}\right] = \nabla^2 h(\mathbf{r},t) \tag{S10}$$

$$\frac{\partial}{\partial t}\left[\frac{\delta c_+(\mathbf{r},t)}{D_+} - \frac{\delta c_-(\mathbf{r},t)}{D_-}\right] = \nabla^2 g(\mathbf{r},t) - \frac{2\tilde{z}^2e^2}{\varepsilon_o\varepsilon k_BT}\langle c\rangle g(\mathbf{r},t) \tag{S11}$$

Ionic current is given by the relation

$$\tilde{z}e\frac{\partial g(\mathbf{r},t)}{\partial t} = -\nabla_{\mathbf{r}}\cdot I(\mathbf{r},t) \tag{S12}$$

which is obtained from Eqs. S1 and S4. In order to compute the current, we consider two limiting cases of near symmetric and highly asymmetric diffusion in the following.

Near symmetric diffusion: $D_+ \simeq D_-$

Note that Eqs. S10- S11 can be written as

$$\frac{\partial}{\partial t}\left[\left\{\frac{1}{D_+}+\frac{1}{D_-}\right\}h(\mathbf{r},t) + \left\{\frac{1}{D_+}-\frac{1}{D_-}\right\}g(\mathbf{r},t)\right] = 2\nabla^2 h(\mathbf{r},t) \tag{S13}$$

$$\frac{\partial}{\partial t}\left[\left\{\frac{1}{D_+}-\frac{1}{D_-}\right\}h(\mathbf{r},t) + \left\{\frac{1}{D_+}+\frac{1}{D_-}\right\}g(\mathbf{r},t)\right] = 2\left[\nabla^2-\kappa^2\right]g(\mathbf{r},t) \tag{S14}$$

where $\kappa^2 = \frac{2\tilde{z}^2e^2}{\varepsilon_o\varepsilon k_BT}\langle c\rangle$.

For $D_+ \simeq D_-$, we can neglect the terms with prefactor of $\frac{1}{D_+} - \frac{1}{D_-}$ in the above equations.

Neglecting these terms, we get

$$\frac{\partial h(\mathbf{r},t)}{\partial t} = \frac{2D_+D_-}{D_+ + D_-}\nabla^2 h(\mathbf{r},t) \tag{S15}$$

$$\frac{\partial g(\mathbf{r},t)}{\partial t} = \frac{2D_+D_-}{D_+ + D_-}\left[\nabla^2 g(\mathbf{r},t) - \kappa^2 g(\mathbf{r},t)\right] \tag{S16}$$

Highly asymmetric diffusion: $D_+ \ll D_-$ **and** $D_+ \to 0$

In this case, we can take the approximation that slow moving species is in steady state in contrast to the other moving species i.e., we assume that $\frac{\partial \delta c_+ \mathbf{r},t)}{\partial t} = 0$ in Eqs. S10- S11. This approximation allows us to write $g(\mathbf{r},t)$ in the form (cf. Eq. S11)

$$\frac{\partial g(\mathbf{r},t)}{\partial t} = D_-\left[\nabla^2 - \kappa^2\right] g(\mathbf{r},t) \tag{S17}$$

along with the relation $2\nabla^2 \delta c_+(\mathbf{r},t) = \kappa^2 g(\mathbf{r},t)$.

The above two limiting cases reveal that for the calculation of ionic current, we need to solve

$$\frac{\partial g(\mathbf{r},t)}{\partial t} = D\left[\nabla^2 - \kappa^2\right] g(\mathbf{r},t) \tag{S18}$$

where $D = 2D_+D_-/(D_+ + D_-)$ for the near symmetric diffusion case and $D = D_-$ for the highly asymmetric diffusion. For one dimensional variation along z axis in charge density, we consider a current blocking metallic electrode so that flux is zero at the surface and solution containing ions at concentration $\langle c \rangle$ far from the electrode. A zero flux condition at the surface leads to the boundary condition for charge as $\left[\frac{\partial g}{\partial z}\right]_{z=0} = -\frac{\kappa^2 Q}{\tilde{z}e}$, where Q is the surface charge density. With these boundary conditions, the solution of Eq. S18 can be obtained using the Laplace transformation and is given by

$$g(z,t) = \frac{\kappa Q}{2\tilde{z}e}\left\{\exp\left[-\kappa z\right]\mathrm{erfc}\left[\overline{z} - \overline{t}\right] - \exp\left[\kappa z\right]\mathrm{erfc}\left[\overline{z} + \overline{t}\right]\right\} \tag{S19}$$

where $\overline{z} = \frac{z}{2\sqrt{Dt}}, \overline{t} = \sqrt{\kappa^2 Dt}$ and erfc is the complementary error function ($= 1 - \mathrm{erf}$, erf being the

error function). For the one-dimensional system, current per unit area becomes (cf. Eq. S12)

$$\tilde{z}e\frac{\partial g(z,t)}{\partial t} = -\frac{\partial I(z,t)}{\partial z} \tag{S20}$$

which can be readily integrated over z ranging from ∞ to any arbitrary value of $z = z_0$. The integration gives

$$I(z_0,t) = I(\infty,t) + \kappa^2 QD\exp\left[-\kappa^2 Dt\right]\left[1-\mathrm{Erf}\left[\frac{z_0}{\sqrt{2Dt}}\right]\right] \tag{S21}$$

As the current is collected by the electrode at $z = 0$, we have used Eq. S21 for $z_0 = 0$ for comparison with experimental results. For $z_0 = 0$, Eq. S21 becomes

$$I(0,t) = I(\infty,t) + \frac{Q}{\tau}\exp\left[-\frac{t}{\tau}\right] \tag{S22}$$

where we have introduced a characteristic time (τ) for charging in the form $\tau = 1/\left[\kappa^2 D\right]$.

For $t \gg \tau$, $I(0,t) = I(\infty,t)$ i.e., the current becomes independent of location. Also, if the current becomes independent of time (t) we can construct the so-called steady state values for given system parameters. In the following, we present a steady state analysis for current and write it as a function of the local electrostatic potential for the one-dimensional system.

Steady state analysis for one dimensional system

At steady state, $I_i(\mathbf{r},t) \equiv I_i$ i.e., current becomes independent of location and time, which, in turn, means that $\frac{\partial c_i(\mathbf{r},t)}{\partial t} = 0$. For one dimensional variation in the electrostatic potential along z direction, we need to solve for flux given by (cf. Eq. S2)

$$\mathbf{J}_i(\mathbf{r},t) \equiv \mathbf{J}_i(z) = -D_i\left[\frac{\partial c_i(z)}{\partial z} + \frac{z_i e}{k_B T}c_i(z)\frac{\partial \psi(z)}{\partial z}\right] \tag{S23}$$

where we have used $\xi_i = z_i e D_i / k_B T, c_i(\mathbf{r},t) \equiv c_i(z), \psi(\mathbf{r},t) \equiv \psi(z)$ and $c_i(z)$ is the number of ions of type i per unit volume. Using Eqs. S4 and S23, the equation for current can be written as

$$\begin{aligned} \mathbf{I}_i(\mathbf{r},t) &\equiv \mathbf{I}_i(z) = -z_i e D_i \left[\frac{\partial c_i(z)}{\partial z} + \frac{z_i e}{k_B T} c_i(z) \frac{\partial \psi(z)}{\partial z} \right] \\ &= -z_i e D_i \exp\left[-\frac{z_i e \psi(z)}{k_B T} \right] \frac{\partial}{\partial z} \left\{ c_i(z) \exp\left[\frac{z_i e \psi(z)}{k_B T} \right] \right\} \end{aligned} \tag{S24}$$

For steady state $\mathbf{I}_i(z) = I_i$, this equation can be readily intergrated over the thickness of the film $(= L)$ to give

$$I_i = -z_i e D_i \frac{c_i(L) \exp\left[\frac{z_i e \psi(L)}{k_B T} \right] - c_i(0) \exp\left[\frac{z_i e \psi(0)}{k_B T} \right]}{\int_0^L dz \exp\left[\frac{z_i e \psi(z)}{k_B T} \right]} \tag{S25}$$

Comparison with experiments

In order to extract information regarding concentration of ions on each side of the film, we use Eq. S25 to fit the experimental data for steady state current as a function of applied voltage. For the experiments done on films containing the polymerized ionic liquid, voltage bias is applied locally using an AFM tip and the electrostatic potential inside the film can be inferred by solving the standard electrostatic problem for a given tip geometry and appropriate boundary conditions. Due to the fact that the electrostatic potential depends on the tip geometry, the current-voltage relation also depends on the tip geometry via Eq. S25.

In this work, we use the fact that the effects of applied bias are most prominent near the tip. Thus, we use a Taylor expansion around the location of tip apex to write the electrostatic potential as

$$\psi(z) = \psi(0) + \left[\frac{\partial \psi(z)}{\partial z} \right]_{z=0} z + \frac{1}{2} \left[\frac{\partial^2 \psi(z)}{\partial z^2} \right]_{z=0} z^2 \tag{S26}$$

The functional form for the coefficients, $\frac{\partial \psi(z)}{\partial z}$ and $\frac{\partial^2 \psi(z)}{\partial z^2}$ at the tip apex can be inferred by approximating the tip as an hyperboloid. Solving the Laplace equation for a hyperboloid-plane geometry

so that the apex is at $z = a$ from $z = 0$ plane, the electrostatic potential is given by

$$\psi(z) = \psi(a) + \frac{\psi(0) - \psi(a)}{\ln\left[\frac{c-a}{c+a}\right]} \left[\ln\left[\frac{1+\zeta}{1-\zeta}\right] + \ln\left[\frac{c-a}{c+a}\right]\right] \tag{S27}$$

where the hyperboloid is defined by

$$\frac{z^2}{a^2} - \frac{r^2}{b^2} = 1 \tag{S28}$$

so that $r^2 = y^2 + x^2$ is the radial co-ordinate. Also, $c^2 = a^2 + b^2$ and

$$2\zeta^2 = 1 + \frac{r^2+z^2}{c^2} - \sqrt{\left[1 + \frac{r^2+z^2}{c^2}\right]^2 - \frac{4z^2}{c^2}} \tag{S29}$$

Using Eqs. S27 and S29, $\frac{\partial \psi(z)}{\partial z}$ and $\frac{\partial^2 \psi(z)}{\partial z^2}$ at the tip apex (i.e., $z = a, r = 0$) are given by

$$\left[\frac{\partial \psi(z)}{\partial z}\right]_{z=a} = \frac{2c}{c^2 - a^2} \frac{\psi(a) - \psi(0)}{\ln\left[\frac{c+a}{c-a}\right]} \tag{S30}$$

$$\left[\frac{\partial^2 \psi(z)}{\partial z^2}\right]_{z=a} = \frac{4ac}{c\left(c^2 - a^2\right)^2} \frac{\psi(a) - \psi(0)}{\ln\left[\frac{c+a}{c-a}\right]} \tag{S31}$$

Note that $-\frac{\partial \psi(z)}{\partial z}$ is the electric field along positive z-axis. For $[\psi(a) - \psi(0)] > 0, \frac{\partial \psi(z)}{\partial z} > 0$ at $z = a$, which means that the electric field lines point away from the apex (i.e., along negative z-axis).

We use Eqs. S30 and S31 to infer the functional form of expansion coefficients in Eq. S26. Switching back to the original coordinate system so that the tip apex is at $z = 0$ and z-axis point away from the apex, we get

$$\left[\frac{\partial \psi(z)}{\partial z}\right]_{z=0} = -\Gamma_1 \left[\psi(0) - \psi(L)\right] \tag{S32}$$

$$\left[\frac{\partial^2 \psi(z)}{\partial z^2}\right]_{z=0} = \Gamma_2 \left[\psi(0) - \psi(L)\right] \tag{S33}$$

where $\Gamma_1 > 0$ and $\Gamma_2 > 0$ are parameters, which depend on tip geometry. Note that the negative sign in front of Γ_1 originates from the fact that electric field is in the direction of positive z axis (i.e., pointing away from apex) when we switch direction of z axis and shift the origin of coordinate system to the tip apex. Mathematically, it results from rotation of the axes by 180 degrees, which leads to a change of sign for $\partial/\partial z$ and doesn't affect $\partial^2/\partial z^2$.

Plugging Eqs. S26, S32 and S33 in Eq. S25, using $z_i = -1$ for the counterion and assuming $\psi(0) > \psi(L)$, the contribution to current coming from transport of counterions is

$$I_{i=-} = 2eD_i\sqrt{\frac{\Gamma_2 V_m}{\pi}}\exp\left[-\Gamma^2 V_m\right]\frac{\{c_i(L)\exp[V_m] - c_i(0)\}}{\mathrm{erf}\left[\Gamma\sqrt{V_m}\right] - \mathrm{erf}\left[\left(\Gamma - L\sqrt{\Gamma_2}\right)\sqrt{V_m}\right]} \tag{S34}$$

where $\Gamma = \frac{\Gamma_1}{2\sqrt{\Gamma_2}}$ and $V_m = e\left[\psi(0) - \psi(L)\right]/k_BT$.

Similarly, plugging $z_i = +1$ for ions on the polymer backbone and evaluating the integral over z, the contribution to current coming from transport of positive ions (i.e., $i = +$) is

$$I_{i=+} = eD_i\frac{\sqrt{\Gamma_2 V_m}\{c_i(L)\exp[-V_m] - c_i(0)\}}{\mathrm{DawsonF}\left[\Gamma\sqrt{V_m}\right] - \exp\left[-L(\Gamma_1 - \Gamma_2 L)V_m\right]\mathrm{DawsonF}\left[\left(\Gamma - L\sqrt{\Gamma_2}\right)\sqrt{V_m}\right]} \tag{S35}$$

where DawsonF is the Dawson integral.

The net current is $I = \sum_{i=+,-} I_i$. In the limit of $\psi(0) - \psi(L) \to 0, c_i(0) \simeq c_i(L) = c_i$, the net current is given by

$$I = \sum_{i=\pm} I_i = \sum_{i=\pm}\frac{e^2 D_i c_i}{Lk_BT}\left[\psi(0) - \psi(L)\right] \tag{S36}$$

which is in agreement with Ohm's law and defines ionic conductivity of $i-$ type ions as $\sigma_i = \frac{e^2 D_i c_i}{k_BT}$.

For estimating the concentration of ions on each side of the film, we have assumed that the diffusion constant of ions on the polymer backbone is much less than that of counterions and the contribution to ionic current is mainly coming from transport of counterions. Keeping Γ_1, Γ_2 fixed while fitting different experimental data sets using Eq. S34, in principle, we can estimate the

concentration of ions on each side of the film. However, no satisfactory fits were obtained using this protocol. In order to demonstrate this, we have presented one such comparison between the experimental data and the current-voltage relation based on Eq. S34 in Figure S4. Furthermore, the fits were found to be insensitive to the concentration of ions (cf. Figure S4) and film thickness (data not shown) due to the presence of large terms in the exponents ($= V_m$) especially in the non-linear regime for applied voltages > 5 V. This shortcoming of the PNP model to describe experimental data has led us to look for alternative mechanisms and formalism. In the next section, we present such a formalism where the dissociation of ion-pairs into "free" ions (or charge carriers) is taken into account and coupled with the PNP formalism.

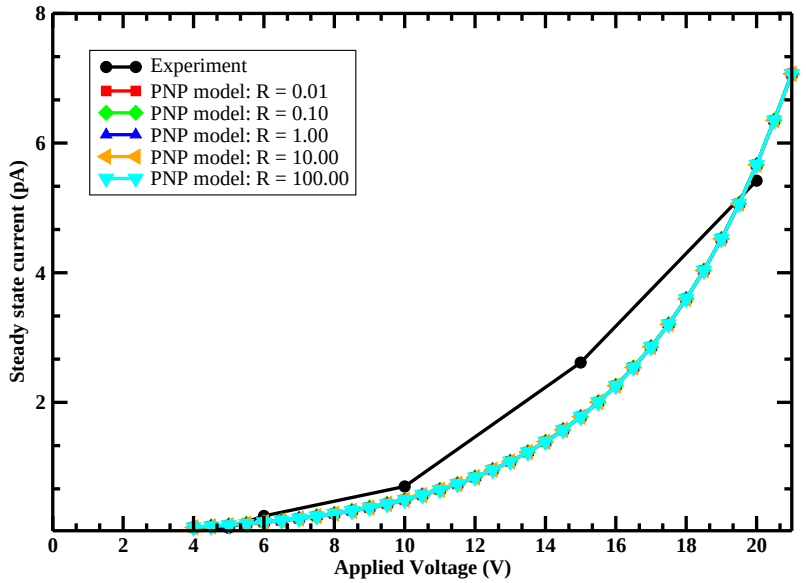

Figure S4: Modeling of experimental data on the steady state current using Eq. S34, derived from the PNP model is shown here. $\Gamma, L\sqrt{\Gamma_2}, R = c_-(0)/c_-(L)$ and $\frac{2}{\sqrt{\pi}} eD_- c_-(L)/L$ are chosen as the fitting parameters. Plots shown above, based on Eq. S34, are obtained by fixing $\Gamma = 1.016, L\sqrt{\Gamma_2} = 0.825, \frac{2}{\sqrt{\pi}} eD_- c_-(L)/L = 7.672 \times 10^{-4}$ and varying R. Insensitivity of the current-voltage relation based on Eq. S34 highlight the unphysical nature of the PNP model for the strong electric fields, in particular.

Wien-Onsager extension of the PNP formalism

In order to extract information regarding the concentration of "free" ions in the film, we use Eq. S34 to fit the experimental data for current as a function of voltage. Comparison of the obtained current-voltage relations are found to be insensitive to the concentration of ions at high voltage biases due to the exponentials in the numerators (cf. S34). Such a shortcoming of the theoretical formalism can be circumvented if one considers the fact that mobile ion concentration changes with applied voltage bias due to the dissociation of ion-pairs (the Wien effect[4–6]). In this work, we merge Onsager's theory of the Wien effect with the PNP formalism as follows. Noting that the effects of applied bias are most prominent near the tip, we use a Taylor expansion around location of the tip apex to write the electrostatic potential as

$$\psi(z) \quad = \quad \psi(0) + \left[\frac{\partial \psi(z)}{\partial z}\right]_{z=0} z \tag{S37}$$

This is the same as the approximation of constant electric field inside the film. In other words, we ignore the non-linear spatial dependence of electrostatic potential inside the film due to double layer formation. The electric field at the tip apex, i.e., $E_0 = -\frac{\partial \psi(x)}{\partial x}$ can be inferred by approximating the tip as an hyperboloid or by comparison of theory and experimental results on the kinetics of charging. Plugging Eq. S37 in Eq. S25, the net steady state current per unit area is

$$I = \sum_{i=\pm} I_i \quad = \quad \left[\sum_{i=\pm} \frac{z_i^2 e^2 D_i c_i}{k_B T}\right] E_0 \tag{S38}$$

which is the Ohm's law.

However, it is to be noted that the linear dependence of current on the applied electric field as described by Eq. S38 is only observed at weak electric fields. Non-linear relation between the current and voltage can be introduced into Eq. S38 if we use the Onsager's steady state theory[6] of ionic dissociation in an applied electric field. Such a treatment leads to the same equation Eq.

S38 with the replacement of c_i by $c_i(E_0)$ so that

$$c_i(E_0) \quad = \quad \alpha(E_0)c_p = \frac{K(0)G(E_0)}{2}\left[\sqrt{1+\frac{4c_p}{K(0)G(E_0)}}-1\right] \tag{S39}$$

and

$$G(E_0) \quad = \quad \frac{I_1\left[2\sqrt{l_B e|E_0|/k_BT}\right]}{\sqrt{l_B e|E_0|/k_BT}} \tag{S40}$$

where I_1 is the modified Bessel function of order one (not to be confused with the symbol I_i for current). $K(0)$ is the dissociation constant in the absence of an applied electric field, c_p is the initial concentration of ion-pairs and $\alpha(E_0)$ is the electric field dependent degree of ionization. Note, here only the magnitude of E_0 ($=|E_0|$) appears in the theory and direction of the electric field doesn't play a role.

Comparison between the theory and experimental results on the steady state current reveals that Eqs. S38, S39 and S40 describe the experimental data remarkably well. In particular, for the comparison with data on the current as a function of *surface charge*, we use $\sum_{i=\pm}\frac{z_i^2e^2D_ic_p}{\varepsilon k_BT}$,$c_p/K(0)$ and $l_Be^2/S\varepsilon k_BT$, S being the area of the tip-surface junction (assumed to be equal to the area of tip apex), as fitting parameters. Noting that $K(0)G(E_0)$ is the dissociation constant in the presence of an electric field, we can determine the degree of ionization in the PolyIL film for different voltage biases using Eq. S39. Furthermore, it is well-known that presence of ions can lead to change in colligative properties such as the melting point. In order to understand the origin of softening of PolyIL films under an applied voltage, we have estimated the change in melting point resulting from the dissociation of ions, as presented in the next section.

Depression of melting point

The thermodynamic definition of melting point[7,8] of a pure solid relies on equality of chemical potential at the solid-liquid transition temperature. The melting point of solid or equivalently the

freezing point of liquid changes due to presence of "free" ions that influences the chemical potential of the liquid. If we consider polymer chains so that each chain has N repeats then the chemical potential *per repeat* in the solid state (e.g., a crystal) (μ_c^0) at temperature T is

$$\mu_c^0 = h_c^0 - Ts_c^0 \tag{S41}$$

where h_c^0 and s_c^0 are the enthalpy and entropy per repeat, respectively. Similarly, the chemical potential per repeat in the liquid state can be written as

$$\mu_l^0 = h_l^0 - Ts_l^0 \tag{S42}$$

where the subscript l stands for "liquid". At the melting temperature, $T = T_m^0$, $\mu_c^0 = \mu_l^0$, which leads to the thermodynamic definiton of melting point of one component polymeric system as

$$T_m^0 = \frac{h_l^0 - h_c^0}{s_l^0 - s_c^0} = \frac{\Delta h}{\Delta s} \tag{S43}$$

where we have defined $\Delta h = h_l^0 - h_c^0, \Delta s = s_l^0 - s_c^0$.

In the presence of a small amount of a second component such as counterions, the chemical potential of a crystallizable component (e.g., polymer backbones in the case of polymerized ionic liquid) changes, which leads to a shift of melting point of the two component system. In order to understand the effects of concentration of counterions and applied electric field on the shift of the melting point, we consider a two component system containing charged polymer chains and counterions. If the shifted melting temperature is $T = T_m$, then equating chemical potential of a repeat in the solid and liquid state leads to

$$\mu_c^p = h_c^p - T_m s_c^p = \mu_l^p = h_l^p - T_m s_l^p \tag{S44}$$

where superscript p represents "polymer in the mixed phase", the crystallizable component. As

we are interested in quantifying the shift of melting point of mixture from that of pure state, we can subtract the chemical potential in the pure liquid state from both sides, which leads to

$$\mu_c^p - \mu_l^0 \;=\; h_c^p - h_l^0 - T_m(s_c^p - s_l^0) = \left[\mu_l^p - \mu_l^0\right]_{T=T_m} \tag{S45}$$

Using Eq. S43 to eliminate change in entropy, we get

$$-\Delta h^p \left[1 - \frac{T_m}{T_m^0}\right] \;=\; \left[\mu_l^p - \mu_l^0\right]_{T=T_m} \tag{S46}$$

where $\Delta h^p = h_l^0 - h_c^p$. This can be written as

$$\frac{1}{T_m} - \frac{1}{T_m^0} \;=\; -\frac{k_B}{\Delta h^p}\left[\frac{\mu_l^p - \mu_l^0}{k_B T}\right]_{T=T_m} \tag{S47}$$

For a given concentration of "free" ions, the excess chemical potential per repeat can be approximated by[9]

$$\frac{\mu_l^p - \mu_l^0}{k_B T} \;=\; \ln(1-\alpha(E_0)) - \frac{\bar{\kappa}(E_0)^2 a^2}{8\pi\phi}\left[\frac{\bar{\kappa}(E_0)a}{(1+\bar{\kappa}(E_0)a)} + 2\ln(1+\bar{\kappa}(E_0)a)\right] \tag{S48}$$

where $\phi = c_p \pi a^3/6$ is the volume fraction of ion-pairs (which is equal to the volume fraction of monomers) and $\bar{\kappa}(E_0)^2 = 4\pi l_B \alpha(E_0) c_p$, $l_B = e^2/4\pi\varepsilon k_B T$ and a being the diameter of ions. In Eq. S48, $\alpha(E_0)$ is the degree of ionization which depends on the electric field. Plugging Eq. S48 in Eq. S47, a non-linear equation for T_m is obtained. First of all, note that if the temperature dependence of the right hand side in Eq. S48 is suppressed, then it is negative. This means that $T_m < T_m^0$ as $\Delta h^p > 0$ (cf. Eq. S47). Hence, there is a depression of melting point resulting from the presence of ions and the depression is stronger if the concentration of ions increases. So, it is clear from Eqs. S47 and S48 that an applied electric field may shift the melting point due to change of Debye-Hückel screening length resulting from shifts in the ion dissociation equilibrium.

However, Eqs. S47 and S48 results in a non-linear equation to be solved for T_m for a given

T_m^0 and Δh^p. The temperature dependence of the excess chemical potential (cf. S48) arises due to l_B/a, which is the Bjerrum parameter for ion-pairing. In the estimation of the changes in melting point, we have taken l_B/a to be inversely proportional to temperature and ignored the temperature dependence of the relative permittivity.

The Bjerrum parameter at room temperature is determined by equating $c_p/K(0)$ determined by our synergistic experiment-theory work on the charge transport to different theories. We have used two theories, namely the Bjerrum-Fuoss-Kraus[10,11](BFK) and the Ebeling-Grigo[12,13] (EG) expressions for the dissociation constant to infer the parameter l_B/a at room temperature. Inverse temperature dependence of the parameter is used to infer its value at other temperatures. Eq. S39 is used to compute the degree of ionization for different temperatures and estimate the extent of depression in the melting point. In both the theories,

$$\frac{c_p}{K(0)} = \phi P(l_B/a) \tag{S49}$$

where the function $P(l_B/a)$ is given by

$$P(x) \equiv P_{BFK}(x) = 4x^3\left[e^2 - Ei(-2) + Ei(-x) - \frac{e^x}{x}\left\{1+\frac{1}{x}+\frac{2}{x^2}\right\}\right] \tag{S50}$$

in the BFK[10,11] theory so that Ei is the exponential integral. In the EG[13] theory,

$$P(x) \equiv P_{EG}(x) = 48\left[\frac{x^3}{12}\{Ei(x) - Ei(-x)\} - \frac{1}{3}\cosh x - \frac{x}{6}\sinh x - \frac{x^2}{6}\cosh x + \frac{1}{3} + \frac{x^2}{2}\right] \tag{S51}$$

References

(1) Sangoro, J. R., Kremer, F. Acc. Chem. Res. **2012**, 45, 525.

(2) Sangoro, J. Colloid Polym Sci **2014**, 1-6. DOI: 10.1007/s00396-014-3299-4

(3) Muthukumar, M., *Polymer Translocation*; (CRC Press, Boca Raton,FL, 2011).

(4) Wien, M., Phys. Zeits. **1928**, 29, 751.

(5) Wien, M., Phys. Zeits. **1931**,32, 545.

(6) Onsager,L., J. Chem. Phys. **1934**, 2, 599.

(7) Flory, P.J.; *Principles of Polymer Chemistry*; (Cornell University Press, New York, 1953).

(8) Nishi, T.; Wang, T. T., Macromolecules **1975**, 8 (6), 909-915.

(9) Pitzer,K.S., J. Phys. Chem. **1973**, 77, 268.

(10) Fuoss, R.M.; Accascina,F., *Electrolytic Conductance*; (Interscience Publishers, Inc., New York, 1959).

(11) Fuoss,R.M.; Kraus,C.A., J. Am. Chem. Soc. **1933**, 55, 1019.

(12) Yokoyama,H.; Yamatera,H., Bulletin of the Chemical Society of Japan **1975**, 48, 1770.

(13) Ebeling, W.; Grigo, M., Annalen Der Physik **1980**, 37 (1), 21-30.